THEORETICAL ANALYSIS OF A ROUND NOSE TOOL CUTTING AT SMALL DEPTHS

by

MICHAEL A. JETER

B.S., Kansas State University, 1975

A MASTER'S THESIS

Submitted in Partial Fulfillment of the

Requirements for the Degree

MASTER OF SCIENCE

Department of Mechanical Engineering

Kansas State University

Manhattan, Kansas

1979

Approved by:

F. C. Appl

Major Professor

TABLE OF CONTENTS

LIST OF TABLES

LIST OF FIGURES

LIST OF FIGURES (Continued)

NOMENCLATURE

a	Tool radius
h	Depth of cut
P_o	Maximum normal stress on equivalent indenter
b_e	Contact width of equivalent indenter
P_n	Normal load per inch on equivalent indenter
E	Modulas of elasticity of workpiece
R_e	Radius of equivalent indenter
R_o	Radius of workpiece before indentation of equivalent indenter
k	Yield shear stress of workpiece
μ	Coefficient of friction between workpiece and equivalent indenter
μ_2	Coefficient of friction between workpiece and tool
ν	Poisson's ratio
γ	Angle of inclination of equivalent indenter
T_1	Displacement of the workpiece by the equivalent indenter at the intersection of the tool and the elastic-plastic boundary
T_2	Displacement of the workpiece by the tool at the intersection of the tool and the elastic-plastic boundary
P_G	Normal pressure on tool edge at a point G
τ_G	Shear force on tool edge at a point G
P_{1v}	Load per inch of equivalent indenter (vertical with respect to the finished workpiece surface)
P_{1h}	Load per inch of equivalent indenter (horizontal with respect to the finished workpiece surface)

P_{2v} Load per inch of tool in the elastic region (vertical with respect to the finished workpiece surface)

P_{2h} Load per inch of tool in the elastic region (horizontal with respect to the finished workpiece surface)

INTRODUCTION

For many years, the chip forming process in metal cutting had been assumed to be like the standard cutting theory shown in Figure 1. It was assumed that the tool could be approximated as being infinitely sharp and that the chip was formed along a line of concentrated shear. For larger depths of cut this was reasonable since the effects of the rounded tool tip is secondary and often negligible. However, as the depth of cut decreases the effect of the rounded tool tip increases. Recently, it has become apparent that in some situations the effect of the rounded tool tip plays an important role. In the study of wear, for example, it is significant due to the need to know the stress distribution along the tool edge. It has also been noted to play a major role in finish machining [1] and grinding [2]. Due to the growing recognition of this problem, it is felt that research in this area is of prime importance.

When considering small depths of cut, the action that exists around a rounded tool tip is a very complex process. Besides the complications due to the tool geometry and material properties, the process includes a region of plastically flowing material that exists in conjunction with a region of elastically deforming material. In plasticity, this is referred to as a "constrained plastic flow problem" and is one of the most difficult types. The stress-strain relations and compatibility equations that evolve are difficult to handle, and very few complete solutions are found. Most of

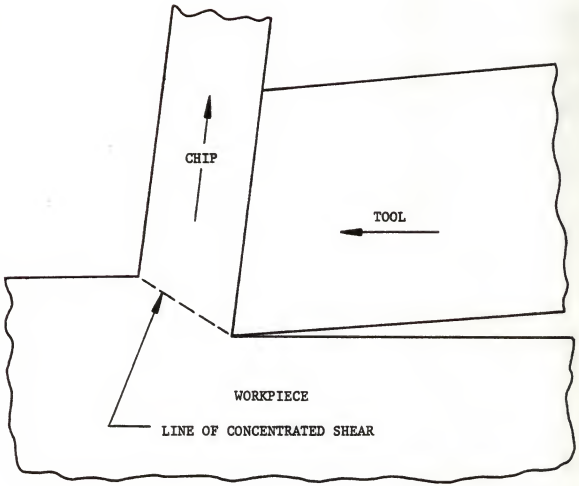

MODEL OF STANDARD CUTTING THEORY

Figure 1

the work done in this area has been done by using various types of approximations. Abdelmoneim and Scrutton [1] derived an expression for the specific cutting energy in terms of the undeformed chip thickness and tool radius. They modeled the process by assuming the tool edge to be subject to a rubbing action at and beneath a portion of the curved tool base. Above that, they assumed the base is subject to a cutting action. Shaw [2] and Goyen [3] both modeled the cutting process as an extrusion type process. Shaw assumed a relationship between the cutting process and a new hardness indentation theory he had developed. He then derived the specific cutting energy based on the undeformed chip thickness, tool radius, and two terms he developed within his indentation theory. Goyen developed a method to determine the geometry of the cutting process based on an approximation of the pressure distribution along a line in the elastic region of his cutting model. He was then able to calculate the pressure distribution along the tool edge based on the geometry and the material properties of the workpiece.

It was the object of this work to investigate the chip forming process around the rounded portion of a tool tip cutting at a very small depth. Since the problem is of a complex nature and a direct mathematical approach was believed not practical, it was felt that an approximation of the cutting process would again be a more feasible approach. It was decided that the approximation should take the form of a mathematical model that included the effects of the blunt nose of the tool and also the compatibility of the elastic and plastic regions of the workpiece. The model was developed to determine the force required by the tool in terms of the shape of the tool, known properties of the workpiece, and a given depth of cut. With this

capability, the model could be applied to a specific cutting case, the results compared to experimental data, and conclusions drawn as to the accuracy of the model.

The model developed was based partially on the work presented by Goyen. His model seemed to most successfully integrate the elastic and plastic regions together, and also seemed to define the chip forming process logically. Numerical results were obtained from the theoretical model and compared to experimental results obtained by Abdelmoneim and Scrutton.

DEFINITION OF THE PROBLEM

The cutting conditions at the tip of a round nose tool, cutting at small depths, was modeled as a two dimensional plain strain problem, as shown in Figure 2. The tool was considered to be a rigid cylinder of infinite length having a velocity vector of V_t. The workpiece was imagined as a half space being elastically, and plastically, displaced by the tool. Mathematically, the workpiece material was modeled as elastic, perfectly plastic [4], Figure 3, and it was assumed that it had homogeneous and isotropic properties. In the plastic region it was also assumed that the properties were not affected by hydrostatic pressure and that the elastic strain was negligible. Chip formation was conceived to be at a velocity of V_c, and the result of an extrusion process where the tool and the elastic-plastic boundary acted as die walls. It was also assumed that the chip formation was steady state and not affected by temperature or dynamics. Along the tool face in the plastic region there was believed to exist an important point called the "stagnation point." This point was considered to be the place where the material separated and flowed either into the forming chip or underneath the tool. Under actual cutting conditions, it was believed that a "dead metal zone" might exist at the stagnation point. However, to simplify the cutting model it was assumed the dead metal zone did not exist. Although this limited the application of the model to workpiece material that showed little tendencies for dead metal zones, it was felt necessary due to the complexity of the build-up.

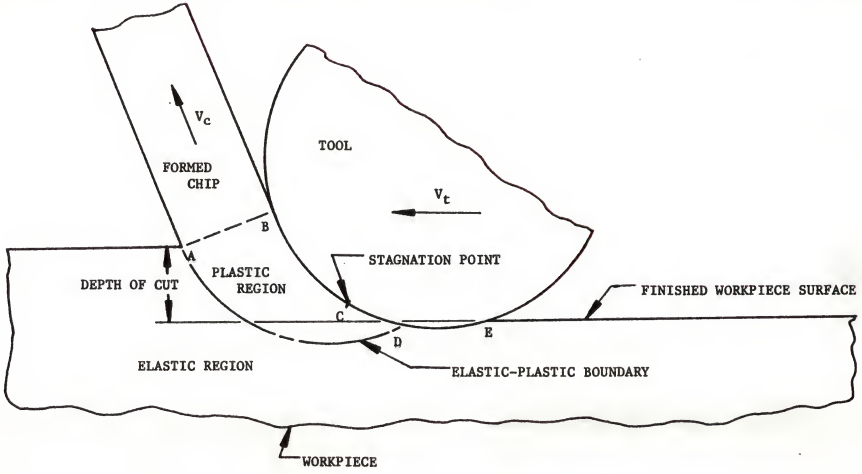

MODEL - ROUND NOSE TOOL CUTTING AT SMALL DEPTHS

FIGURE 2

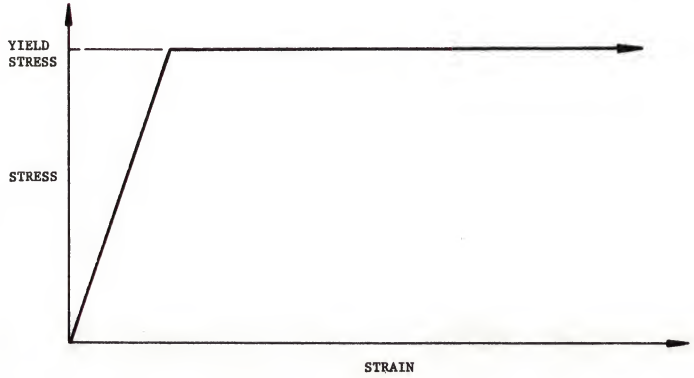

STRESS-STRAIN RELATION FOR ELASTIC, PERFECTLY PLASTIC MATERIAL

FIGURE 3

With the model developed to this point, the chip forming process was described in general but lacked sufficient information to determine the specific geometric condition and force requirements of a specific cutting case. To overcome this problem an analytical aid was added to the model in the form of an "equivalent indenter." It was conceived as a rigid cylindrical indenter that elastically deformed the workpiece the same amount as the cutting process, Figure 4. The equivalent indenter was geometrically restricted by the cutting process with the pressure along the indenter's edge being governed by the geometry of the cutting process and the workpiece material properties. The equivalent indenter was used in the approximation of the location of the stagnation point and the approximation of the pressure distribution along the tool's edge in the elastic region. Along the tool's edge in the plastic region, the pressure distribution was based on the cutting process geometry and workpiece material properties. By assuming the formed chip to be stress free, it was determined that the force required by the tool had to equal the force required by the equivalent indenter. With this assumption and requiring the work done by the tool to be a minimum, it was found that there was only one geometric shape for the cutting process that would satisfy the above conditions. Once the geometric shape of the cutting process was found the force requirements of the tool could be obtained.

To handle the computations required by the mathematical model a computer program was developed (APPENDIX A). As input, it required the depth of cut, the tool point radius, and properties of the workpiece material. With these values, it then determined the proper geometry and the cutting force required per unit length of tool. The basic steps of the analysis used were to first determine a possible geometric configuration for the model, then determine

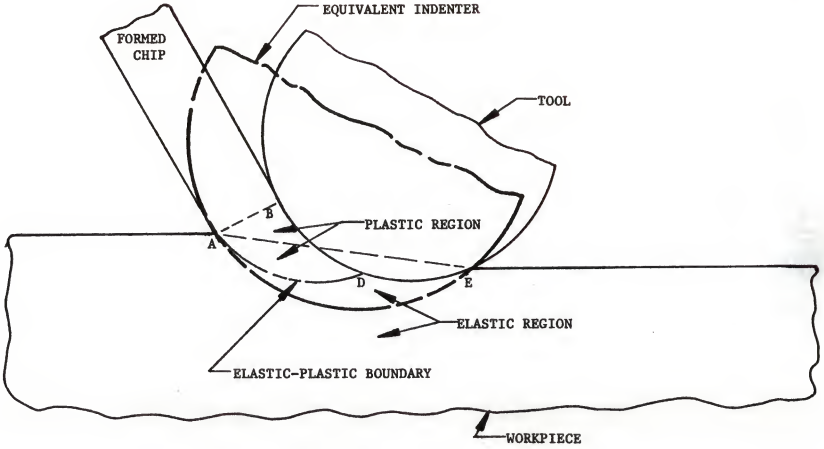

CUTTING MODEL - WITH EQUIVALENT INDENTER

FIGURE 4

the pressure distribution along the tool and along the equivalent indenter. Next, the geometry of the model was varied until the forces required by the tool and the equivalent indenter were equal and the work done by the tool was at a minimum.

Work done by Poritsky [5], which was later worked out numerically by Hamilton and Goodman [6], was used to approximate the equivalent indenter. Poritsky had investigated two cylindrical bodies in sliding contact. He assumed the pressure distribution to be a "Hertzian" elliptical normal distribution with a superposed proportional tangential shearing traction. It was believed that the equivalent indenter could reasonably be represented by a sliding cylindrical indenter that created this type of distribution. Therefore, it was assumed the equivalent indenter had a Hertzian elliptical distribution normal to line AE, Figure 4, with a proportional superposed shearing traction. With the equivalent indenter located close to the elastic-plastic boundary it was also assumed that the equivalent indenter would deform the workpiece to the point of yielding. The normal pressure distribution on the indenter was determined by the application of the Hertz theory for contact between two bodies with the stress at the center of the surfaces in contact being determined from information presented by Hamilton and Goodman. The relationship between the normal and tangential forces was assumed to be constant.

To determine the pressure distribution along the tool edge, it was first necessary to locate the intersection of the elastic-plastic boundary with the tool. The criteria used to locate this point was based on the physical limitations and the close relationship that existed between the equivalent indenter and the tool. It was felt that the displacement of the workpiece

by the tool, and the equivalent indenter, would be related with the values being approximately equal around the point of interest. Therefore, it was assumed that the point of intersection between the elastic-plastic boundary and the tool would be on a line perpendicular to the workpiece surface where the tool and the equivalent indenter elastically displaced the workpiece material the same amount, Figure 5. The elastic region was assumed to exist only where the tool displaced the workpiece material less than the equivalent indenter. The point of intersection was limited to below the surface represented by the finished surface. This eliminated the possibility of the elastically deformed material not recovering completely.

The pressure distribution along the tool edge was determined in two sections, the elastic and plastic regions. The tool edge along the plastic region was analyzed by applying work presented by Schneider and Cheatham [7]. They presented equations that determined the pressure beneath a general punch profile, dependent only on the terminal points of the slip-line field. It was assumed that all the slip-lines crossed the stress free line $\overline{AB}$, into the stress free chip, at a $\pi/4$ radians angle as determined by Tresca or von Mises yield criteria [4]. To determine the angle of intersection of the slip-lines with the tool, it was necessary to assume a friction relationship between the tool and the workpiece. Results from a theoretical model for friction in metal working by Wanhiem and Petersen [8] were used. The stagnation point was assumed to be where the slip-line intersected the tool at $\pi/4$ radians. Since the flow above the stagnation point was determined to go into the chip and below the stagnation point under the tool, it was assumed that the shear stresses in the tool were as shown in Figure 6. Along the tool edge, in the elastic region, it was assumed that the pressure distribution was the same

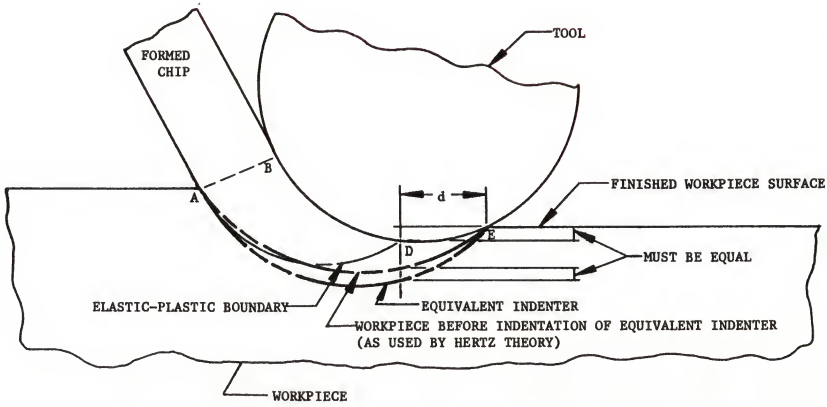

INTERSECTION OF ELASTIC-PLASTIC BOUNDARY WITH TOOL

FIGURE 5

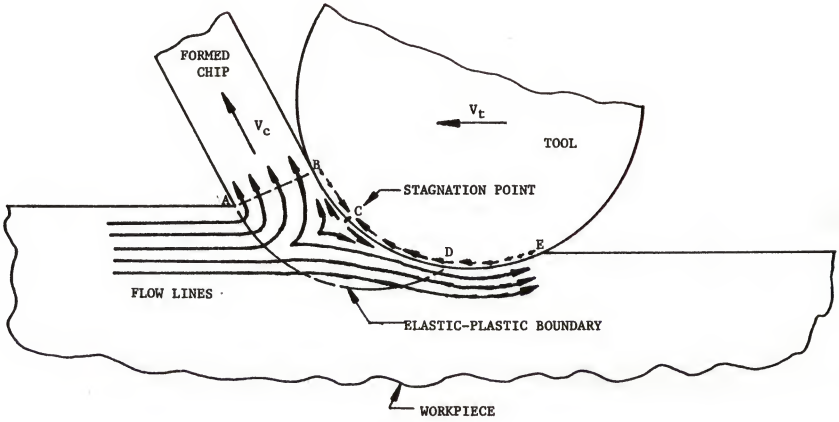

SHEARING FORCE ON TOOL

FIGURE 6

as the pressure distribution along the equivalent indenter. This was assumed to be reasonable due to the close relationship between the tool and the indenter.

THE EQUIVALENT INDENTER

As previously discussed, the pressure distribution on the equivalent indenter was assumed to be a normal Hertzian elliptical distribution with a proportional tangential shearing traction. The maximum stress between the workpiece and the equivalent indenter was assumed to be great enough in magnitude to deform the workpiece to the point of yielding. It was felt that this pressure distribution depicted a reasonable approximation to the actual distribution and also presented an elementary method of analysis.

The normal pressure distribution for the equivalent indenter was determined by Hertz theory of contact between two bodies [9]. For line contact between two cylinders of infinite length

$$P' = \tfrac{1}{2}\pi b\, P_o \tag{1}$$

where

$$b = \frac{4\, P_o \left(\dfrac{1-\nu_1^2}{E_1} + \dfrac{1-\nu_2^2}{E_2}\right)}{\dfrac{1}{R_1} + \dfrac{1}{R_2}}, \tag{2}$$

where P' is the load per unit length in the normal direction, P_o is the maximum normal stress, b is the width of contact, ν is Poisson's ratio, E is the modulas of elasticity, and R is the radius of curvature. The subscripts "1" and "2" refer to the separate cylinders.

The equivalent indenter with Hertz theory was incorporated in the model, as shown in Figure 7. It was required that the equivalent indenter intersect the workpiece surface at points A and E, and lie only in the elastic region. Although the shape of the elastic-plastic boundary was unknown, the intersection of it and the stress free line $\overline{AB}$ was determined to cross at an angle of $\pi/4$ radians. It was assumed that the equivalent indenter would not intrude on the plastic region if it intersected line $\overline{AB}$ at an angle greater than or equal to $\pi/4$ radians. In the model it was required that the equivalent indenter intersect line $\overline{AB}$ at $\pi/4$ radians. The radius of curvature of the equivalent indenter and the workpiece material before indentation were defined as R_e and R_o, respectively, while the width of the contact was defined as b_e. The cylindrical indenter was assumed rigid and therefore the modulus of elasticity was infinite. When the Hertz theory was combined with the model, equation (1) became:

$$P_n = \tfrac{1}{4}\pi b_e P_o \tag{3}$$

and equation (2) became:

$$b_e = \frac{4 P_o \left(\frac{1-\nu^2}{E}\right)}{\frac{1}{R_e} + \frac{1}{R_o}} , \tag{4}$$

P_n being the normal load per inch on the equivalent indenter. The values of R_e, R_o, and b_e were determined when a possible geometric condition was assumed, E and ν were assumed known since they were properties of the workpiece.

The magnitude of P_o was determined from information presented by Hamilton and Goodman [6]. They had numerically worked out equations, which were

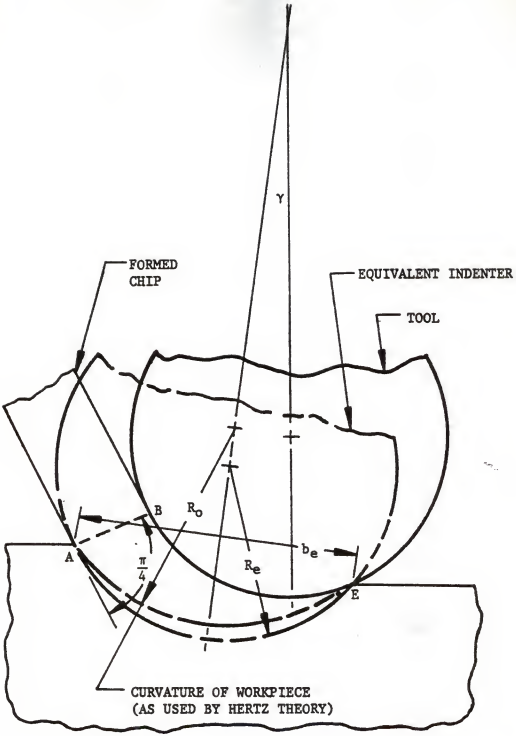

CUTTING MODEL-NOMENCLATURE

FIGURE 7

developed by Poritsky [5], for the stress fields of two cylinders in sliding line contact. Poritsky had determined the equations assuming the pressure distribution between the cylinders to be Hertzian elliptical with Hamilton and Goodman applying the equations requiring Poisson's ratio for the cylinders to equal 0.3 and the point of maximum stress in the stress fields to be at the yield point as determined by von Mises yield criteria. Hamilton and Goodman developed three stress fields, μ equal to 0.0, 0.25 and 0.50, which showed that:

$$P_o' = k' \cdot f(\mu') \tag{5}$$

where P_o' was the maximum pressure between the two cylinders, k' the yield shear stress of the cylinder, and $f(\mu')$ a function of the coefficient of friction, μ', between the cylinders. It was assumed that P_o, the maximum normal pressure between the workpiece material and the equivalent identer could be determined by:

$$P_o = k \cdot f(\mu) \tag{6}$$

where k is the yield shear stress of the workpiece, and $f(\mu)$ is the same as $f(\mu')$ in equation (5) except that the coefficient of friction, μ, is between the equivalent indenter and the workpiece.

When equation (6) was incorporated into the mathematical model it was necessary to determine a continuous function for $f(\mu)$. It was chosen to approximate the continuous function because of its complex origin. The continuous function was approximated by ploting a line, with respect to the coefficient of friction, μ, through the three known points determined from the work presented by Hamilton and Goodman, and requiring it to follow a

lower bound of $f'(\mu)$, Figure 8. The lower bound, $f'(\mu)$, was developed by assuming the element at the point of yielding would not yield before the element shown in Figure 9. By applying von Mises yield criteria to the element shown in Figure 9, it is determined that

$$f'(\mu) = \frac{1}{\left[\mu^2 + 1/3\ (1.0 - \frac{\nu + \nu^2}{1-\nu^2})^2\right]^{\frac{1}{2}}} \quad . \tag{7}$$

Poisson's ratio, ν, was assumed to equal 0.3.

With the normal load per inch determined for the equivalent indenter, the tangential shearing traction, P_t, was easily obtained by:

$$P_t = \mu P_n \ . \tag{8}$$

Since the work done by the tool was determined to be in the direction parallel to the workpiece surface, it was chosen to rotate the forces determined for the equivalent indenter to these axes. The vertical load per inch for the equivalent indenter, P_{1v}, was determined by:

$$P_{1v} = P_n \cos(\gamma) - P_t \sin(\gamma), \tag{9}$$

and the horizontal load per inch, P_{1h}, by:

$$P_{1h} = P_n \sin(\gamma) - P_t \cos(\gamma). \tag{10}$$

The angle γ was the amount the axes were rotated, Figure 7.

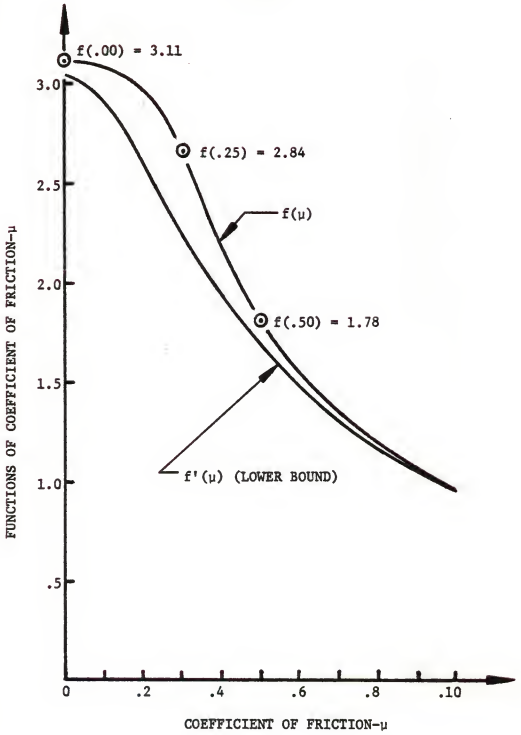

CONTINUOUS FUNCTIONS OF THE COEFFICIENT OF FRICTION

FIGURE 8

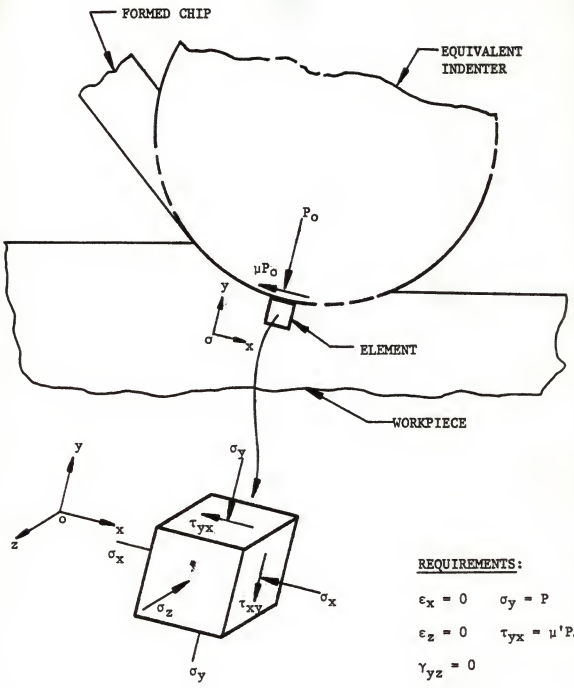

ELEMENT USED TO DETERMINE LOWER BOUND-$f'(\mu)$

FIGURE 9

THE TOOL

To determine the pressure distribution along the tool edge, the analysis was divided into the elastic and plastic regions. In the elastic region, the pressure distribution was assumed to be approximately that along the adjacent equivalent indenter, while in the plastic region, the pressure distribution and the location of the stagnation point were determined by work presented by Schneider and Cheatham. The location of the point where the elastic-plastic boundary intersected the tool was approximated by assuming that the tool and the equivalent indenter displaced the workpiece material the same amount. It was also required that along the elastic region the tool displaced the workpiece material less than the equivalent indenter. Although this analysis was only an approximation of the pressure distribution, it was felt to be reasonable.

Before the analysis of the elastic or plastic regions could be completed, it was necessary to locate the point of intersection between the tool and the elastic-plastic boundary. The point was assumed to lie on a vertical line where the tool and the equivalent indenter displaced the workpiece material the same amount, Figure 10. Since the distance from the line to the intersection of the tool with the workpiece surface, distance d, could not be determined directly, it was found by minimizing the difference between the two displacements T_1 and T_2. The magnitudes of T_1, the displacement of the workpiece by the equivalent indenter, and T_2, the displacement of the workpiece by the tool, were determined by:

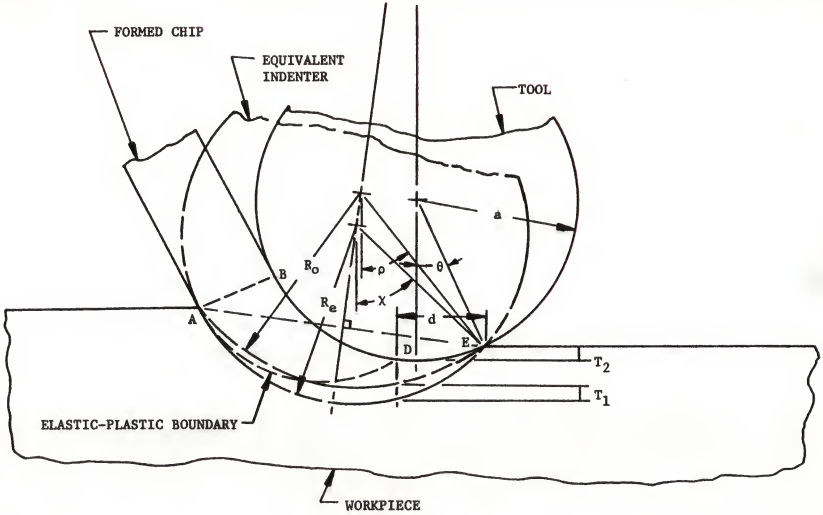

CUTTING MODEL-NOMENCLATURE

FIGURE 10

$$T_1 = R_o([1.0 - (\frac{d}{R_o} - \sin \rho)^2]^{\frac{1}{2}} - \cos \rho) - R_e([1.0 - (\frac{d}{R_e} - \sin \chi)^2]^{\frac{1}{2}} - \cos \chi) \tag{11}$$

and

$$T_2 = a([1.0 - (\frac{d}{a} - \sin \theta)^2]^{\frac{1}{2}} - \cos \theta). \tag{12}$$

It was chosen to limit the point of intersection between the tool and the elastic-plastic boundary to below the workpiece surface since it would imply that the workpiece material did not completely recover elastically if the point was above it. To insure this, d was limited by:

$$0 \leq d \leq 2.0 \text{ a } \sin \theta, \tag{13}$$

where, a, was the tool radius. It was determined that for d to be greater than zero, θ had to be greater than $\chi-\rho$. This also insured that the equivalent indenter displaced the workpiece material more than the tool elastic region.

The normal pressure distribution along the tool edge in the elastic region was assumed to be equivalent to that of the adjacent equivalent indenter. The force required per inch of tool in the elastic region was determined by integrating the pressure distribution over the adjacent region of the equivalent indenter and then calculating the proportional shearing stress, assuming the coefficient of friction to be that between the tool and the workpiece. The resulting forces were then rotated to be normal and tangent to the workpiece surface. The integration resulted in the force, perpendicular to line $\overline{AE}$, P_{2N}, being:

$$P_{2N} = \frac{P_o\, b_e}{\pi} (\phi - \sin \phi \cos \phi) \tag{14}$$

where

$$\phi = \cos^{-1} (1.0 - \frac{2.0\, d}{b_e \cos \gamma}) \tag{15}$$

and the superposed tangential shearing force, P_{2t}, to be:

$$P_{2t} = \mu_2 P_{2N} , \tag{16}$$

where μ_2 is the maximum theoretical coefficient of friction between the tool and the workpiece material as determined by Wanhiem and Petersen [8], Figure 11. The forces were rotated to the horizontal and vertical axes with respect to the workpiece surface, by:

$$P_{2h} = P_{2N} \cos \gamma - P_{2t} \sin \gamma \tag{17}$$

and

$$P_{2v} = P_{2N} \sin \gamma - P_{2t} \cos \gamma , \tag{18}$$

P_{2h} and P_{2v} being the horizontal and vertical forces required by the elastic region of the tool and γ being the amount of rotation.

The calculations of the pressure distribution along the tool in the plastic region were determined from work presented by Schneider and Cheatham. They presented a theory which stated that the pressure at a point on a rigid punch indenting a rigid, perfectly plastic material could be determined uniquely from the boundary stresses and the relative angles between the tangents to the slip line at the punch and the boundary, Figure 12. The normal pressure, P_m, on the punch being:

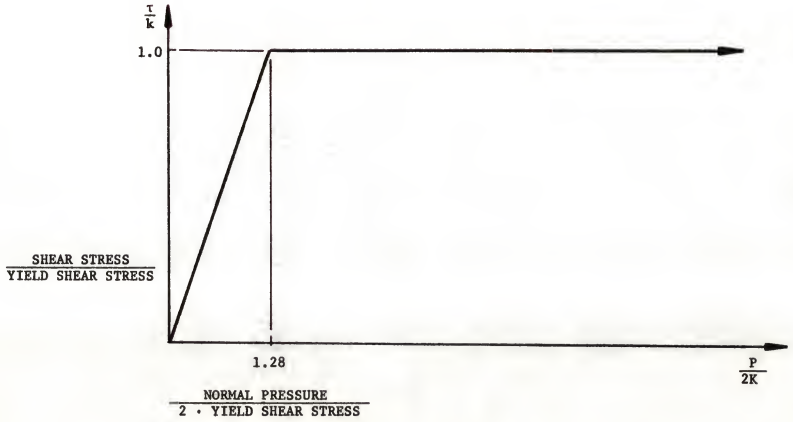

FRICTION BETWEEN WORKPIECE AND TOOL

FIGURE 11

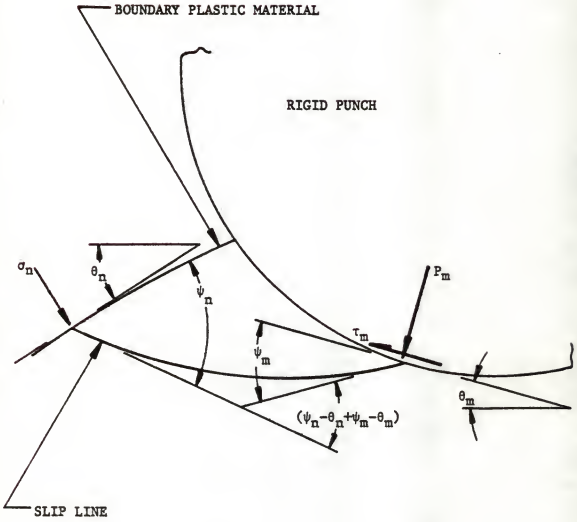

RIGID PUNCH INDENTING RIGID, PERFECTLY PLASTIC MATERIAL-NOMENCLATURE

FIGURE 12

$$P_m = \sigma_n + k \sin 2\psi_m + k \sin 2\psi_n + 2k\ (\psi_n - \theta_n + \psi_m - \theta_m) \qquad (19)$$

and the tangential shearing traction, τ_m, being:

$$\tau_m = -k \cos \psi_m \ . \qquad (20)$$

The normal pressure at the intersection of the boundary with the slip line was represented by σ_n, while k represented the yield stress in shear of the plastic material. Equation (19) was adapted to the model as shown in Figure 13. The line $\overline{AB}$ was considered a stress free surface since the forming chip was considered stress free. By applying von Mises or Tresca yield criteria, it was determined that the slip lines would intersect the line $\overline{AB}$ at a $\pi/4$ radians angle. Assuming line $\overline{AB}$ to be stress free, equation (19) becomes:

$$P_G = k + k \sin 2\psi_G + 2k\ (\frac{\pi}{4} - \zeta + \psi_G - \Lambda) \qquad (21)$$

and equation (20) becomes:

$$\tau_G = -k \cos 2\psi_G \ , \qquad (22)$$

where P_G is the normal pressure, τ_G, is the shear force, ψ_G, the angle of intersection between the slip line and the tool, and Λ the location of point G on the tool edge. To determine the angle ψ_G, it was required that:

$$T_G = \mu_2 P_G \ , \qquad (23)$$

where μ_2 is the coefficient of friction between the tool and the workpiece.

The point where the slip line crossed the tool at a $\pi/4$ radians angle was assumed to be the stagnation point. This was determined since the calculations of the pressure distribution along the tool edge resulted in a continuous function and for the shearing stress, τ_G, to change sign it must

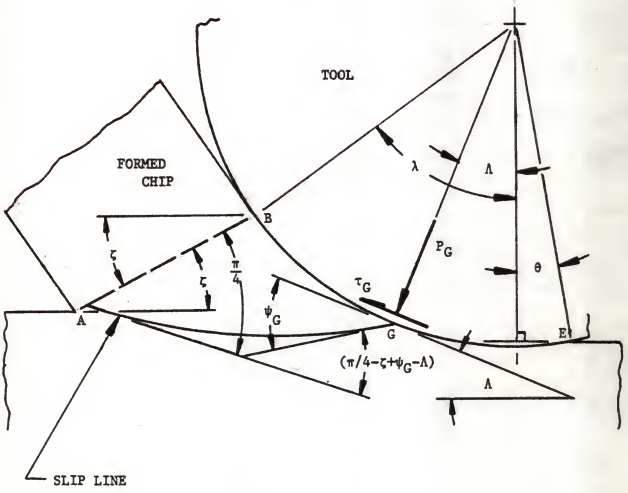

CUTTING MODEL-NOMENCLATURE

FIGURE 13

pass through the point where τ_G equals zero. From equation (22) it was determined that τ_G equals zero when ψ_G equals $\pi/4$ radians. To determine the forces required per inch of tool in the plastic region, the pressure distribution was numerically integrated by use of Simpson's rule.

RESULTS

To aid in the evaluation of the cutting model developed, the model was applied to specific cutting cases which had been experimentally investigated. The data chosen to compare results with were obtained by Abdelmoneim and Scrutton [1]. It was chosen because the metal used showed little tendency for a dead metal zone, the data were presented such that the information needed by the developed model was easily obtained, and was the same experimental data used by Goyen [3] to evaluate his model. It was felt that a comparison between the model developed in this paper and the model developed by Goyen would be of significance. Goyen had used the same basic method, with an identical equivalent indenter, but had determined differently the location where the tool and the finished workpiece surface intersected, the location of the stagnation point, and the point of intersection between the elastic-plastic boundary and the tool. He had also assumed that there was a flat spot on the lower surface of the tool.

Abdelmoneim and Scrutton had performed experiments which determined the cutting forces required by a negative rake tool having a known point radius of .003 inches. They used high-speed orthogonal tools ground to a specific shape which were then mounted individually into a lathe tool dynamometer, and the experiments performed. Frequent regrinding and low speeds were used to lessen problems due to tool wear. Among other workpiece specimens, they used free cutting brass composed of 61.5% copper, 35.0% zinc and 3.25% lead.

They had determined the yield shear stress of the free cutting brass to be approximately 40.9 x 10^3 psi by sharp tool cutting experiments. This corresponds to 70.8 x 10^3 psi tensile yield stress using von Mises yield criteria. It should be noted that Abdelmoneim and Scrutton presented only the force required by the tool in the direction parallel to the finished workpiece surface. Thus no comparison could be made between the calculated and experimental force required by the tool normal to the finished workpiece surface.

The cutting cases investigated by Abdelmoneim and Scrutton were adapted to the model by letting the values of the tool radius, and the yield tensile stress of the workpiece be .003 inches and 70.8 x 10^3 psi, respectively. It was also assumed that the modulus of elasticity and Poisson's ratio of the workpiece were 14 x 10^6 lbs/in^2 and 0.3, respectively. With these inputs, the computer program was run and the geometry with the force requirements of the tool being determined for a range of depths of cut. As with the model developed by Goyen, it was found that it only worked for a small range of depths. Table I and Figure 14 give the depths of cut for which the program worked with the corresponding dimensions and forces as determined by the model and the experiments. It should be noted that the experimental data given in Table I were determined from an empirical equation given by Abdelmoneim and Scrutton which was based on one hundred sixty-six experimental data points. The resulting geometric conditions and pressure distribution along the edge of the tool are given in Figures 15 thru 18 and Tables II thru V.

TABLE I

EXPERIMENTAL AND CALCULATED VALUES

Depth of Cut	.0005	.0006	.0007	.0008
Tool Radius (in.)	.003	.003	.003	.003
Cutting Model Dimensions				
b_e (see Figure 7) (in.)	.00177	.00194	.00210	.00225
R_e (see Figure 7) (in.)	.00313	.00307	.00308	.00318
R_o (see Figure 7) (in.)	.00331	.00323	.00323	.00333
Formed Chip Thickness (in.)	.000026	.000030	.000036	.000048
Required Tool Force (Tangent to Workpiece Surface)				
Experiment [1] (lb_f)	159.3	178.8	197.0	214.1
Calculated (lb_f)	109.6	125.3	140.1	153.5
Required Tool Force (Normal to Workpiece Surface)				
Calculated (lb_f)	142.2	153.5	162.9	170.8

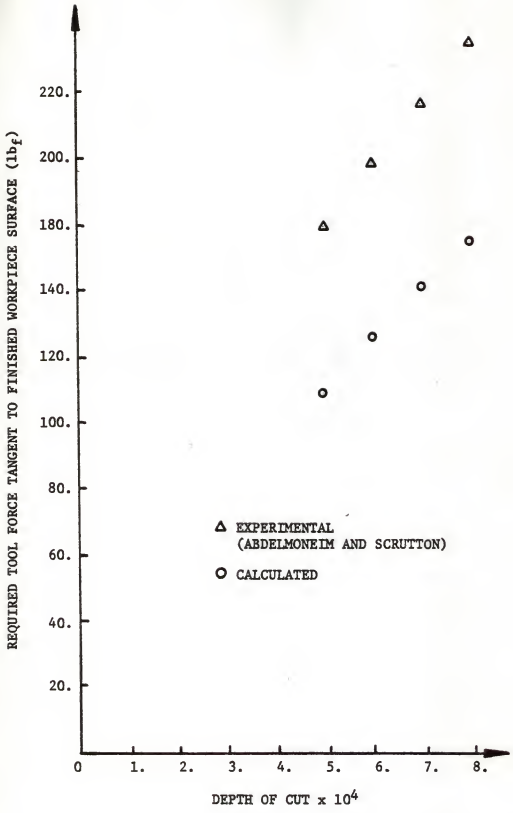

EXPERIMENTAL VERSUS CALCULATED FORCES

FIGURE 14

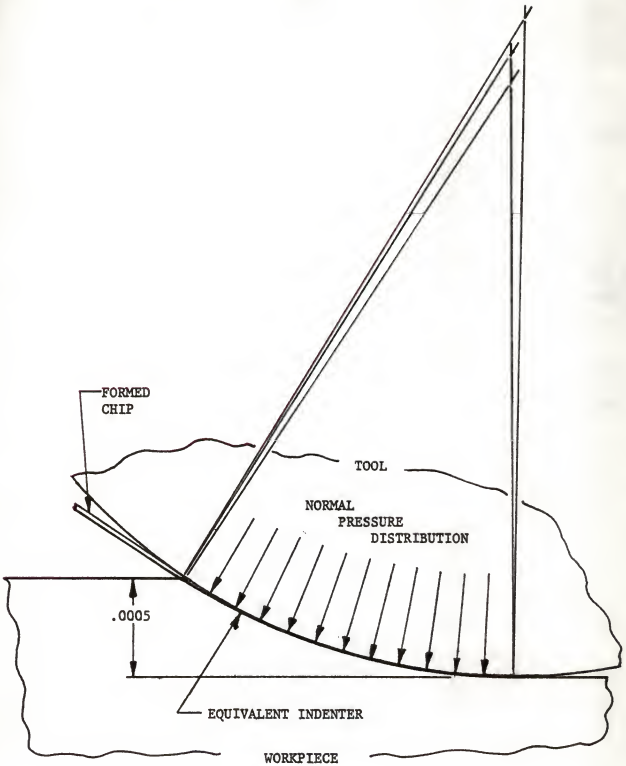

CALCULATED CUTTING MODEL GEOMETRY
(DEPTH OF CUT .0005)

FIGURE 15

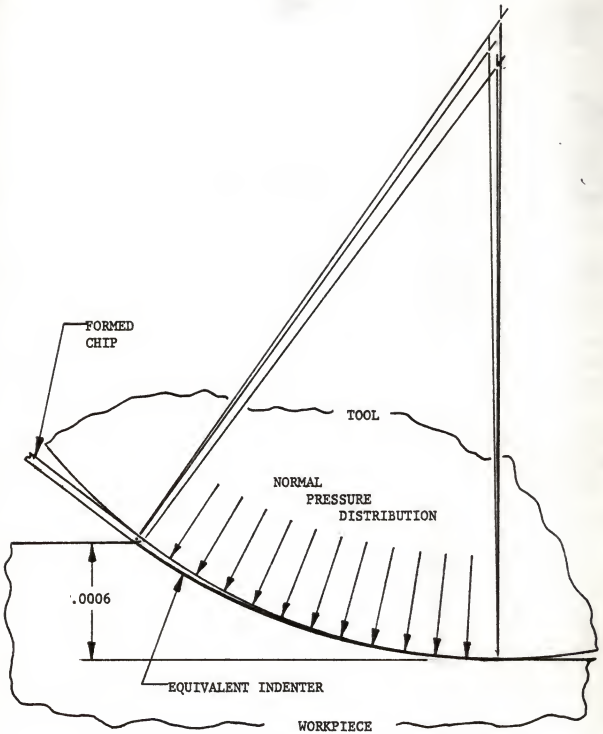

CALCULATED CUTTING MODEL GEOMETRY
(DEPTH OF CUT .0006)

FIGURE 16

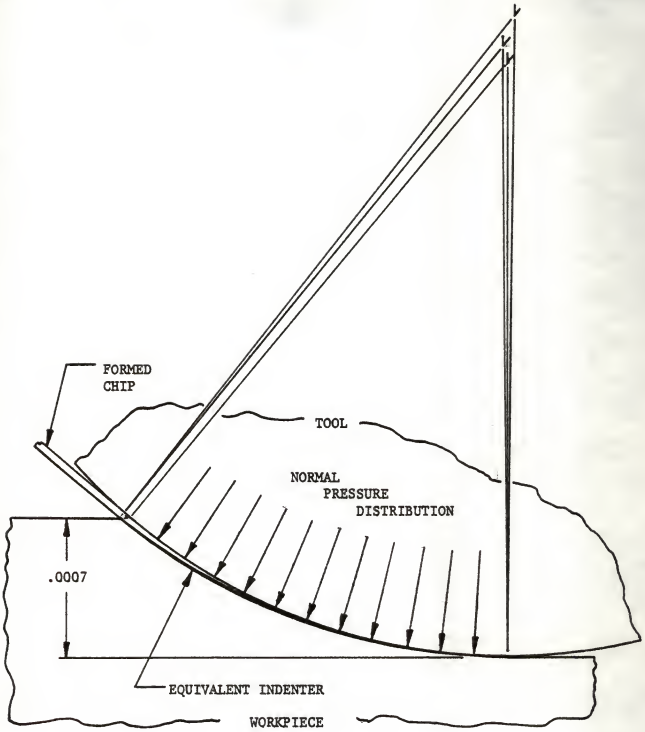

CALCULATED CUTTING MODEL GEOMETRY
(DEPTH OF CUT .0007)

FIGURE 17

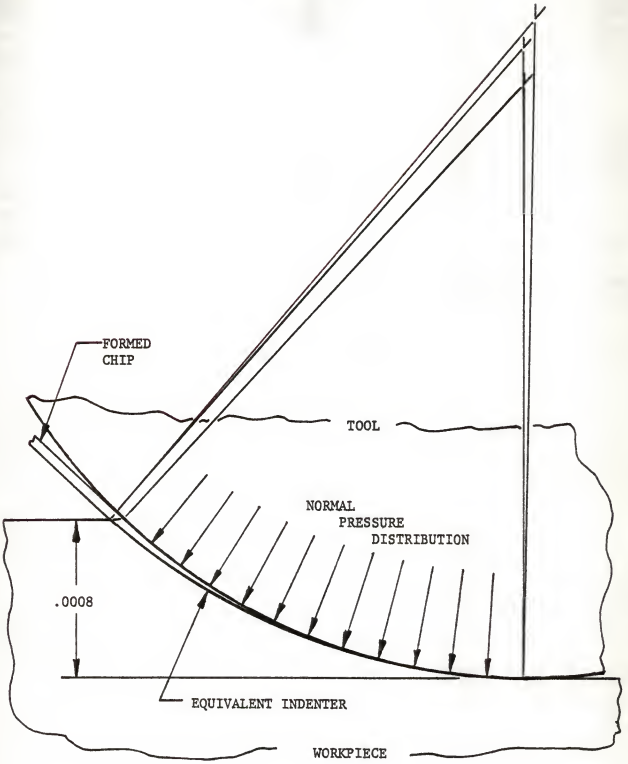

CALCULATED CUTTING MODEL GEOMETRY
(DEPTH OF CUT .0008)

FIGURE 18

TABLE II

STRESS DISTRIBUTION ON TOOL SURFACE
(DEPTH OF CUT .0005)

Λ* (RADIANS)	P_G* ($\times 10^4$ ($lb_f/in.^2$))	τ_G* ($\times 10^4$ ($lb_f/in.^2$))
0.0000	10.255	4.029
.0491	10.240	3.981
.0983	10.158	3.940
.1474	10.039	3.900
.1965	9.913	3.855
.2457	9.790	3.801
.2948	9.663	3.748
.3439	9.496	3.700
.3931	9.365	3.634
.4422	9.193	3.577
.4913	9.025	3.515
.5405	8.735	3.483
.5896	8.490	3.411

* See Figure 13

TABLE III

STRESS DISTRIBUTION ON TOOL SURFACE
(DEPTH OF CUT .0006)

Λ^* (RADIANS)	P_G^* ($\times 10^4$ ($lb_f/in.^2$))	τ_G^* ($\times 10^4$ ($lb_f/in.^2$))
0.0000	10.409	4.049
.0539	10.333	4.019
.1078	10.242	3.984
.1617	10.135	3.942
.2156	10.015	3.896
.2695	9.859	3.845
.3234	9.742	3.790
.3774	9.590	3.730
.4313	9.430	3.668
.4852	9.261	3.602
.5391	9.084	3.533
.5930	8.900	3.462
.6469	8.709	3.388

* See Figure 13

TABLE IV

STRESS DISTRIBUTION ON TOOL SURFACE
(DEPTH OF CUT .0007)

Λ^* (RADIANS)	P_G^* ($\times 10^4$ (lb$_f$/in.^{2}))	τ_G^* ($\times 10^4$ (lb$_f$/in.^{2}))
0.0000	10.464	4.070
.0583	10.401	4.046
.1166	10.317	4.013
.1750	10.213	3.973
.2333	10.093	3.926
.2916	9.959	3.874
.3499	9.811	3.816
.4082	9.651	3.754
.4665	9.481	3.688
.5249	9.301	3.618
.5832	9.111	3.544
.6415	8.913	3.467
.6998	8.706	3.387

* See Figure 13

TABLE V

STRESS DISTRIBUTION ON TOOL SURFACE
(DEPTH OF CUT .0008)

Λ^* (RADIANS)	P_G^* ($\times 10^4$ ($lb_f/in.^2$))	τ_G^* ($\times 10^4$ ($lb_f/in.^2$))
0.0000	10.493	4.081
.0625	10.440	4.061
.1249	10.362	3.030
.1874	10.260	3.991
.2498	10.138	3.944
.3123	9.999	3.889
.3747	9.844	3.829
.4372	9.676	3.764
.4997	9.494	3.693
.5621	9.301	3.618
.6246	9.098	3.539
.6870	8.885	3.456
.7495	8.663	3.370

* See Figure 13

CONCLUSIONS AND DISCUSSION

The object of this research was to investigate the chip forming process around the tip of a tool cutting at very small depths. This was accomplished by modeling the cutting process, then making the model functional, and finally applying the model to experimentally investigated cases. It was hoped that the results would accurately duplicate the experimental data, thus verifying the cutting model.

Though the results did not duplicate the experimental data sufficiently to verify the model, it was felt that the investigation was still useful. The calculated forces required by the tool did match the experimental data well enough to indicate some merit in the principles of the cutting model. More importantly, the investigation did indicate a reason why the results of the model did not more closely duplicate the experimental data. Before these indications can be verified, more research is needed to better define the elastic region of the cutting model.

The comparison of the experimental data with the calculated data showed that the calculated geometry of each cutting process investigated was distorted; and the calculated force tangent to the workpiece surface was approximately 70% of the experimental value. The geometry was considered to be distorted since the formed chip thickness was much thinner than thought to be realistic.

A comparison of the model developed by Goyen and the model developed in this investigation was used to determine the reason for the deviation of

the calculated data from the experimental data. As stated before, the basic methods used by Goyen were applied except that the location where the tool and the finished workpiece surface intersected, the location of the stagnation point, and the point of intersection of the elastic-plastic boundary with the tool were determined differently. The method used to calculate the pressure distribution along the edge of the equivalent indenter and the location of the equivalent indenter were the same. Goyen had assumed that a flat spot existed on the lower surface of the tool, and had calculated cutting forces and geometry conditions for various depths of cut and flat spot sizes. As the size of the flat spot decreased, it was found that the geometry of the tool and the location of the intersection of the tool with the finished workpiece surface approached the results of this investigation. It was also found that as the flat spot size decreased, the formed chip thickness also decreased. For small flat spot sizes, Goyen's results showed unrealistically small chip thicknesses and, for all sizes of flat spots, low calculated force values. Although no direct comparison can be made between the two investigations, a definite relationship between the models and the results can be shown. From this it was concluded that the major source of error in both investigations was probably due to common assumptions. Ignoring errors introduced by assumptions which differ between the two models, and approximations based on some type of theoretical or experimental work, a list of four possible sources of large error was developed, Figure 19. From this list, the assumption that the pressure distribution along the tool's edge in the elastic region was equivalent to the pressure distribution along the adjacent equivalent indenter was eliminated since there was a high level of confidence in the assumption.

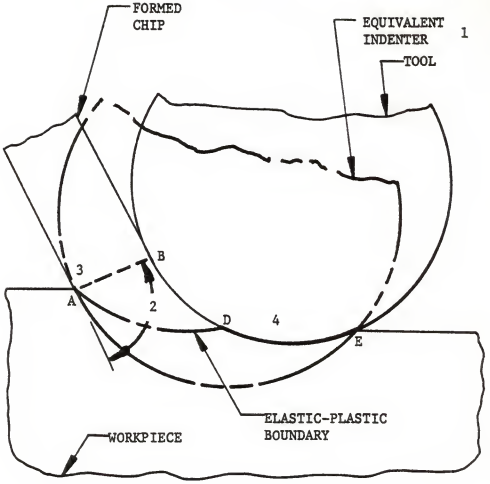

1 Pressure distribution and magnitude along edge of equivalent indenter.

2 Equivalent indenter will lie in the elastic region if this angle is greater than or equal to $\pi/4$ radians.

3 $\overline{AB}$ is stress free.

4 Pressure distribution along the tool's edge in the elastic region is equivalent to that of the adjacent equivalent indenter.

POSSIBLE SOURCES OF ERROR

FIGURE 19

The results of this work indicate that a better approximation of the stress field in the elastic region is needed before an approximate cutting model of this type can be successful. It is felt that a better understanding of the stress distribution, essential boundary conditions, and tendencies of the workpiece material is needed. It is also felt that the best approach to determine a better approximation would be to first develop a more realistic theoretical approximation of the elastic stress field. Although the confidence level in the assumption that line $\overline{AB}$, Figure 19, was stress free is not high enough to eliminate it from the list of possible sources of error, it is felt that the error resulting from the assumption would be small and could initially be ignored.

REFERENCES

1. Abdelmoneim, M. Es., and R. F. Scrutton. "Tool Edge Roundness and Stable Build-Up Formation in Finish Machining," Journal of Engineering for Industry. Transactions of ASME, (November 1974), pp. 1258-1267.

2. Shaw, M. C. "A New Theory of Grinding," Mechanical and Chemical Engineering Transactions of the Institution of Engineers, Australia, Vol. MC8, No. 1, May, 1972, pp. 73-78.

3. Goyen, M. L. "Theory of Cutting with Large Negative Rake Cutting Tools," (Unpublished M.S. Thesis, Kansas State University, 1976).

4. Johnson, W., and Mellor, P.B. Engineering Plasticity, Van Nostrand Reinhold Company, London, 1973.

5. Poritsky, H. "Stresses and Deflections of Cylindrical Bodies in Contact With Application to Contact of Gears and of Locomotive Wheels," Journal of Applied Mechanics. Trans. ASME, vol. 72, 1950, pp. 191-201.

6. Hamilton, G. M., and L. E. Goodman. "The Stress Field Created by a Circular Sliding Contact," Journal of Applied Mechanics. (June 1966), pp. 371-376.

7. Schneider, W. C., and J. B. Cheatham, Jr. "Indentation Analysis for General Shapes of Surface Boundaries and Punch Profiles," Society of Petroleum Engineers Journal. (September 1971), pp. 321-329.

8. Wanheim, T., Bay, N., and Petersen, A. S. "A Theoretically Determined Model for Friction in Metal Working Processes," Wear, Vol. 28, 1974, pp. 251-258.

9. Timoshenko, S., and J. N. Goodier. Theory of Elasticity, 2nd ed. New York: McGraw-Hill Book Company, Inc., 1951.

APPENDIX A

COMPUTER PROGRAM

INTRODUCTION TO THE COMPUTER PROGRAM

The following computer program was written to apply the model developed in this research and determine the forces on a blunt nose tool in a specified cutting case. To define a specific cutting case the program required the modulas of elasticity, yield stress, and Poisson's ratio of the workpiece, along with the tool radius, and the depth of cut. The program worked by assuming the values of four independent variables from which it determined a geometric shape for the cutting process and the forces along the tool's and equivalent indenter's edges. It then varied the independent variables until all the governing conditions for the model were met. It was found that solutions existed for only a small range of depth of cut due to geometric restrictions.

PROGRAM LISTING

```
      IMPLICIT REAL*8(A-H,C-Z,$)
      REAL*8K,MU
      DIMENSION STSZ(4),MATID(4,4),SOL(6),XMU(21),YFMU(21),PT(6)
      DIMENSION BE1(51),TBE1(51),BE2(5),TBE2(5),TEST2(10),D1(10),D2(2)
      DIMENSION PPP(4,5),STPT(5),X5(21),Y5(21),STPT1(5),XX5(5,5)
      DIMENSION IFLAG(6),IC(4),PT1(6),IFLAG2(6)
      COMMON/BLK1/H,A,ZETA,CMEGA,Q,V,RC,P,ASL,RE,GAM,RHO,CHI
      COMMCN/BLK2/SY,K,E,EPS,PC
      COMMON/BLK3/STSZ,MATID
      CCMMCN/BLK4/XMU,YFMU,RMU
      COMMCN/BLK5/DD
      CGMMGN/BLK6/IFLAG
      CGMMON/BLK7/PRR
      H=.00C4
      THA=0.0
      THAE=.0
      MU=.2
      B=.54
      IO(1)=1
      IO(2)=2
      IO(3)=3
      IO(4)=4
      E=140CCOCC.
      A=.003
      SY=70800
      K=SY/(3.**.5)
      EPS=.3
      ASL=.7E54
      RMU=.3E89E5
      DO 10 I=1,21
      J=I-1
   10 XMU(I)=.C5*J
      YFMU(1)=3.106
      YFMU(2)=3.1
      YFMU(3)=3.C8
      YFMU(4)=3.05
      YFMU(5)=2.97
      YFMU(6)=2.841
      YFMU(7)=2.65
      YFMU(8)=2.40
      YFMU(9)=2.16
      YFMU(10)=1.95
      YFMU(11)=1.776
      YFMU(12)=1.64
      YFMU(13)=1.51
      YFMU(14)=1.42
      YFMU(15)=1.33
      YFMU(16)=1.25
      YFMU(17)=1.19
      YFMU(18)=1.12
      YFMU(19)=1.06
      YFMU(2C)=1.00
      YFMU(21)=.95
      DO 20 I=1,4
      STSZ(I)=-.00001
      DO 20 J=1,4
      MATIC(I,J)=0.0
      IF(I.EQ.J) MATID(I,J)=1.0
   20 CONTINUE
      NN=3
```

```
      PT(IC(1))=B
      PT(IC(2))=MU
      PT(IO(3))=THAE
      PT(IO(4))=THA
      PRR=1.
      NN=4
      CALL SCLVE (PT,SCL,IC,NN)
      IF(IFLAG(5).LT. 1) GO TO 50
      CALL SCLVE1(PT,SOL,IC,NN)
      PRR=2.
      CALL CALC(PT,SOL,IO)
   50 CONTINUE
      STOP
      END
      SUBROUTINE SOLVE(PT,SOL,IO,NN)
      IMPLICIT REAL *8 (A-H,C-Z,$)
      DIMENSION STSZ(4),PT(6),TPT(6),MATID(4,4),SOL(6),IO(4),IFLAG(6)
      DIMENSION PPP(4,5),STPT(5),STPT1(5),X5(21),Y5(21),XX5(5,5)
      COMMON/BLK1/H,A,ZETA,OMEGA,Q,V,RC,P,ASL,RE,GAM,RHO,CHI
      COMMON/BLK3/STSZ,MATID
      COMMON/BLK6/IFLAG
      NN2=0
      NN3=0
      DO 11 I=1,5
   11 STPT1(I)=0.0
      Y5(1)=0.0
      CALL CALC(PT,SCL,IC)
      IF(IFLAG(5).LT.0) GO TO-50
      DO 131 I=1,2
  131 IF(DABS(SOL(I)).GT..1    ) GO TO 100
      GO TO 50
  100 CONTINUE
      IF(IFLAG(5).LT.0) GO TO 50
      IJ=0
      DO 101 I=1,4
      IF(IFLAG(I).GT.0) GO TO 101
      IF(IO(I).GT.NN) GO TO 101
      IJ=IJ+1
      STSZ(IC(I))=-.00001
      IF(IFLAG(I).EQ.-2) STSZ(IO(I))= .00001
  101 CONTINUE
      IJ=NN-IJ
      IF(IJ.LT.2.AND.NN3.EQ.1) IFLAG(5)=-3
      IF(IFLAG(5).LT.0) GO TO 50
      IF(IJ.LT.2)NN3=NN3+1
      IF(IJ.GE.2)NN3=0
      NN1=NN+1
      DO 70 J=1,NN
      PPP(J,NN1)=-1.*SCL(J)
      DO 70 I=1,NN
      PPP(J,I)=SCL(J)
      XX5(I,1)=SCL(I)
   70 CONTINUE
      DO 110 J=NN1,6
  110 TPT(J)=PT(J)
      DO 80 I=1,NN
      DO 90 J=1,NN
   90 TPT(J)=PT(J)-MATID(I,J)*STSZ(J)
      CALL CALC(TPT,SCL,IO)
      IF(IFLAG(5).LT.0) GO TO 50
```

```
      DO 132 II=1,2
  132 IF(DABS(SCL(II)).GT..1    ) GO TO 105
      DO 133 II=1,6
  133 PT(II)=TPT(II)
      GO TO 50
  105 CONTINUE
      DO 80 L=1,NN
      PPP(L,I)=(PPP(L,I)-SOL(L))/STSZ(I)
   80 CONTINUE
      CALL GJREC(PPP,PT,STPT,NN)
      DO 151 I=1,NN
      IF(IFLAG(I).LT.0) GO TO 151
      STP=STPT(I)*STPT1(I)
      IF(STP.GE.0.0)GO TO 150
  151 CONTINUE
  152 CONTINUE
      DO 102II=1,4
      IF(IO(II).GT.NN) GO TO 102
      IF(IFLAG(II).GT.0) JJ=IO(II)
  102 CONTINUE
      CO  153 I=2,5
      DI=(I-1)*.25
      Y5(I)=DI
      CO 156 J=1,4
  156 TPT(J)=PT(J)- DI*STPT1(J)
      CALL CALC(TPT,SCL,IO)
      IF(IFLAG(5).LT.0) GO TC 50
      DO 134 II=1,2
  134 IF(DABS(SCL(II)).GT..1    ) GO TO 106
      DO 135 II=1,6
  135 PT(II)=TPT(II)
      GO TO 50
  106 CONTINUE
      DO 153 II=1,NN
      XX5(II,I)=SCL(II)
  153 CONTINUE
      I=JJ
      DO 159 J=1,5
  159 X5(J)=XX5(I,J)
      TTP=0.0
      CALL INTERP(5,5,TTP,STP,X5,Y5,5)
      IF(STP.GT.0..AND.STP.LT.1.0) GO TO 160
      IFLAG(5)=-3
      GO TO 50
  160 CONTINUE
      NN2=NN2+1
      IF(NN2.GT.50) GO TC 50
      DO 154 I=1,5
      PT(I)=PT(I)-STP*STPT1(I)
  154 STPT1(I)=0.0
      GO TO 155
  150 CONTINUE
      DO 157 I=1,NN
      PT (I)=PT(I)+STPT(I)
  157 STPT1(I)=STPT(I)
  155 CONTINUE
      CALL CALC( PT,SCL,IO)
      DO 130 I=1,2
  130 IF(DABS(SCL(I)).GT..1    ) GO TO 100
   50 CONTINUE
```

```
      RETURN
      END
      SUBROUTINE SOLVE1(PT,SCL,IO,NN)
      IMPLICIT REAL*8(A-H,C-Z,$)
      DIMENSION PT(6),SOL(6),IO(4),IFLAG(6),PT1(6)
      COMMON/BLK6/IFLAG
      IK=0
      IN=0
      STP=.005
      CALL SCLVE2(PT,SCL,IC,NN)
      PP=SOL(6)
      IF(IFLAG(4).EQ.-2)STP=-.005
      I1=IFLAG(4)
      DO 11 I=1,6
   11 PT1(I)=PT(I)
   10 CONTINUE
      PT1(4)=PT(4)+STP
      NN=3
      CALL SCLVE(PT1,SCL,IC,NN)
      IF(IFLAG(5).LT.0) GO TO 20
      CALL SCLVE2(PT1,SCL,IC,NN)
      IF(PP.LT.SCL(6)) GO TO 20
      IF(IFLAG(4).LT.0) GO TO 30
      IN=IN+1
      DO 12 I=1,6
   12 PT(I)=PT1(I)
      GO TO 10
   20 CONTINUE
      IF(IN.GT.0) GO TO 30
      IF(IK.GT.0) GO TO 30
      IK=IK+1
      IF(I1.LT.0) GO TO 30
      DO 32 I=1,6
   32 PT1(I)=PT(I)
      STP=-1.*STP
      GO TO 10
   30 CONTINUE
      DO 31 I=1,6
   31 PT(I)=PT1(I)
      RETURN
      END
      SUBROUTINE SCLVE2(PT,SCL,IO,NN)
      IMPLICIT REAL*8(A-H,C-Z,$)
      DIMENSION PT(6),SOL(6),IO(4),IFLAG(6),PT1(6),IFLAG2(6)
      COMMON/BLK6/IFLAG
      NN=2
      IN=0
      DO 11 I=1,6
      IFLAG2(I)=IFLAG(I)
   11 PT1(I)=PT(I)
      PP=SOL(6)
   15 CONTINUE
      IK=0
      IJ=1
      STP=.005
      DO 12 I=1,4
      IF(IO(I).NE.3) GO TO 12
      IF(IFLAG2(I).EQ.-2) STP=-.005
      I1=IFLAG2(I)
      I1=I
```

```
12 CONTINUE
10 CONTINUE
   PT1(3)=PT(3)+STP
   CALL SCLVE(PT1,SCL,IC,NN)
   IF(IFLAG(5).LT.0) GO TO 20
   IF(PP.LT.SOL(6)) GO TO 20
   DO 34 I=1,6
   IFLAG2(I)=IFLAG(I)
34 PT(I)=PT1(I)
   PP=SOL(6)
   IJ=IJ+1
   IF(IFLAG(11).LT.0) GO TO 30
   GO TO 10
20 CONTINUE
   IF(IJ.GT.1) GO TO3C
   IF(IK.GE.1) GO TC30
   IK=IK+1
   IF(II.LT.0) GO TO 30
   DO 41 I=1,6
41 PT1(I)=PT(I)
   STP=-1.*STP
   GO TO 10
30 CONTINUE
   IN=IN+1
   IF(IJ.GT.1) IN=0
   IF(IN.GT.2) GO TO 40
   PT2=PT(3)
   PT(3)=PT(2)
   PT(2)=PT(1)
   PT(1)=PT2
   DO 32 I=1,4
   PT1(I)=PT(I)
   IF(IO(I).EQ.4) GC TO 32
   IO(I)=IO(I)+1
   IF(IC(I).EQ.4) IC(I)=1
32 CONTINUE
   GO TO 15
40 CONTINUE
   SOL(6)=PP
   DO 42 I=1,6
42 IFLAG(I)=IFLAG2(I)
   RETURN
   END
   SUBROUTINE CALC(PT,SCL,IC)
   IMPLICIT REAL*8(A-H,C-Z,$)
   REAL*8K,MU
   DIMENSION PT(6),SCL(6),XMU(21),YFMU(21),IFLAG(6),IO(4)
   COMMON/BLK1/H,A,ZETA,OMEGA,Q,V,RC,P,ASL,RE,GAM,RHO,CHI
   COMMON/BLK2/SY,K,E,EPS,PC
   COMMON/BLK4/XMU,YFMU,RMU
   COMMON/BLK6/IFLAG
   B=PT(IC(1))
   MU=PT(IO(2))
   THAE=PT(IC(3))
   THA=PT(IC(4))
   DO 3 I=1,6
 3 IFLAG(I)=1
   IF(MU.GT.0.0.AND.MU.LT.1.0) GO TC 5
   IF(MU.GE.1.0) GO TO 6
   MU=0.0
```

```
      IFLAG(2)=-1
      GO TO 5
    6 MU=1.0
      IFLAG(2)=-2
    5 CONTINUE
      DO 20 I=1,21
      DC=DABS(MU-XMU(I))
      IF(DC.LT..00000001) GO TO 14
      IF(MU.LT.XMU(I)) GO TO 21
   20 CONTINUE
   21 MM=I+2
      IF(MM.LT.5)MM=5
      IF(MM.GT.21) MM=21
      CALL INTERP(5,MM,MU,FMU,XMU,YFMU,21)
      GO TO 16
   14 CONTINUE
      FMU=YFMU(I)
   16 CONTINUE
      PO=K*FMU
      CALL GECM(THAE,B,THA,BE,D,TEST1)
      IF(IFLAG(6).EQ.-1) CALL THEMN(THAE,B,THA,BE,D,TEST1)
      IF(IFLAG(5).LT.0) GO TO 50
      IF(IFLAG(4).EQ.-3) CALL THAMX(THAE,B,THA,BE,D,TEST1)
      P1P=.25*BE*PO*3.141592653589793
      V=H/BE
      C=(1.-(H/BE)**2)**.5
      CMEGA=DARSIN(D/A-DSIN(THA))
      PHI=2.*DARCOS(1.-2.*C/BE/Q)
      P2P=P1P*(1.- (PHI-DSIN(PHI))/6.283185307179586)
      PY=P2P*(C-RMU*V)
      PX=P2P*(V+RMU*Q)
      N=12
      Z=-1.*ZETA
      IF(CMEGA.GT.Z)GO TO 1
      CALL SINGR(CMEGA,Z,N,XX1,YY1,1)
      CALL SINGR(Z,B ,N,XX2,YY2,2)
      GO TO 10
    1 CALL SINGR(CMEGA,B ,N,XX2,YY2,2)
      XX1=0.0
      YY1=0.0
   10 CONTINUE
      XX=PX -(XX1+XX2)
      YY=PY -(YY1+YY2)
      PXX=XX1+XX2
      PYY=YY1+YY2
      SOL(1)=XX
      SOL(2)=YY
      PPX=P1P*(V+Q*RMU)
      PPY=P1P*(C-V*RMU)
      SOL(3)=(PX**2+PY**2)**.5-(PXX**2+PYY**2)**.5
      SOL(4)=PX/PY-PXX/PYY
      SOL(5)=PPY
      SOL(6)=PPX
      PT(IO(1))=B
      PT(IO(2))=MU
      PT(IO(3))=THAE
      PT(IO(4))=THA
      PT(5)=C
      PT(6)=BE
      PXY=DSQRT(SOL(6)**2+SOL(5)**2)
```

```
      WRITE(6,7)H,A
      WRITE(6,200)PT(IC(4)),PT(6),PT(5),PT(IC(2)),PT(IC(1))
      WRITE(6,300)SOL(1),SCL(2),SOL(3),SOL(6),SCL(5)
      WRITE(6,800)ZETA,CMEGA,PT(IC(3)),ASL,PXY
      WRITE(6,700)RE,RC,RHC,CHI,GAM
    7 FORMAT('0' ,'H=',E15.8,7X,'A=',E15.8)
  200 FORMAT(1X,'THA=',E15.8,5X,'BE=',E15.8,7X,'D=',E15.8,9X,'MU=',E15.8
     1,8X,'LAM=',E15.8)
  300 FORMAT(1X,'TX=',E15.8,6X,'TY=',E15.8,7X,'T1=',E15.8,8X,'PX=',E15.8
     1,8X,'PY=',E15.8)
  700 FORMAT(1X,'RE=',E15.8,6X,'RC=',E15.8,7X,'RHO=',E15.8,7X,'CHI='
     1,E15.8,7X,'GAM=',E15.8)
  800 FORMAT(1X,'ZETA=',E15.8,4X,'CMEGA=',E15.8,4X, 'THAE=',E15.8,6X,
     1'ASL=',E15.8,7X,'PXY=',E15.8)
  801 FORMAT(1X,'IFLAG=',6I3)
   50 CONTINUE
      WRITE(6,801)IFLAG(1),IFLAG(2),IFLAG(3),IFLAG(4),IFLAG(5),IFLAG(6)
      RETURN
      END
      SUBROUTINE GEOM(THAE,B,THA,BE,C,TEST1)
      IMPLICIT REAL*8(A-H,C-Z,$)
      REAL*8K,MU
      DIMENSION BE1(51),TBE1(51),BE2(5),TBE2(5),TEST2(10),D1(10),D2(2)
      DIMENSION IFLAG(6)
      COMMCN/BLK1/H,A,ZETA,CMEGA,Q,V,RC,P,ASL,RE,GAM,RHO,CHI
      COMMCN/BLK2/SY,K,E,EPS,PC
      COMMCN/BLK5/CC
      COMMON/BLK6/IFLAG
      CC(G,W)=G*((1.-(D/G       -DSIN(W))**2)**.5-DCOS(W))
      TEST1=0.0
      D=C.C
      THEMIN=CARSIN(2.*PO*(1.-EPS**2)/E)*1.0000C001
      IF(THAE.GT.THEMIN) GC TC 14
      IFLAG(3)=-1
      THAE=THEMIN
   14 CONTINLE
      IF(H.GT.0.0.AND.H.LT.A) GO TO 17
      IFLAG(5)=-1
      GO TC 55
   17 CONTINUE
      THAMIN=0.0
      IF(THA.GT.THAMIN) GO TC 13
      IFLAG(4)=-1
      THA=THAMIN
   13 CONTINLE
      BMIN=CARCOS(DCOS(THA)-H/A)+.0001
      IF(BMIN.GT.1.57079)IFLAG(4)=-2
      IF(IFLAG(4).EQ.-2)THA=CARCOS(H/A)
      BMIN=CARCCS(DCCS(THA)-H/A)
      IF(B.GT.BMIN) GC TC 15
      IFLAG(1)=-1
      B=BMIN
   15 CONTINLE
      IF(B.LT.1.57C79) GO TO 16
      IFLAG(1)=-2
      B=1.57C79
   16 CONTINUE
      BEMIN=((A*(DSIN(BMIN)+CSIN(THA)))**2+H**2)**.5
      BEMAX=((H**2+(A*(1.+DSIN(THA)+DCOS(THA)/.C00C1)-H/.00001)**2)**.5)
      STEP=(BEMAX-BEMIN)/20.
```

```
      DO 10 I=1,21
      BE1(I)=BEMAX-(I-1)*STEP
      GAM=DARSIN(H/BE1(I))
      ZETA=ASL-GAM-THAE
      IF(ZETA.GT..00001) GO TO 12
      IFLAG(3)=-2
      ZETA=.00001
      THAE=ASL-GAM-ZETA
      IF(THAE.LT.THEMIN) IFLAG(5)=-3
      IF(IFLAG(5).LT.0) GO TO 99
   12 CONTINUE
      Q=((1.-(H/BE1(I))**2)**.5)*BE1(I)
      Q1=(A*(DCOS(THA)-DCOS(B))-H)/DTAN(ZETA)+A*(DSIN(B)+DSIN(THA))
      TBE1(I)=Q-Q1
      IF(DABS(TBE1(I)).LT.1.E-8) GO TO 26
      IF(I.EQ.1) GO TO 10
      TTB=TBE1(I)*TBE1(I-1)
      IF(TTB.LT.0.0) GO TO 11
   10 CONTINUE
   11 BE2(5)=BE1(I)
      BE2(1)=BE1(I-1)
      TBE2(5)=TBE1(I)
      TBE2(1)=TBE1(I-1)
   21 CONTINUE
      STEP=(BE2(5)-BE2(1))/4.
      DO 20 I=2,4
      BE2(I)=BE2(1)+(I-1)*STEP
      GAM=DARSIN(H/BE2(I))
      ZETA=ASL-GAM-THAE
      Q=((1.-(H/BE2(I))**2)**.5)*BE2(I)
      Q1=(A*(DCOS(THA)-DCOS(B))-H)/DTAN(ZETA)+A*(DSIN(B)+DSIN(THA))
      TBE2(I)=Q-Q1
      IF(DABS(TBE2(I)).LT.1.E-8) GO TO 22
   20 CONTINUE
      TT=0.0
      CALL INTERP(5,5,TT,BE,TBE2,BE2,5)
      GAM=DARSIN(H/BE)
      ZETA=ASL-GAM-THAE
      Q=((1.-(H/BE    )**2)**.5)*BE
      Q1=(A*(DCOS(THA)-DCOS(B))-H)/DTAN(ZETA)+A*(DSIN(B)+DSIN(THA))
      TBE=Q-Q1
      IF(DABS(TBE).LT.1.E-8) GO TO 24
      DO 23 I=2,5
      TTB=TBE2(I)*TBE2(I-1)
      IF(TTB.LT.0.0) GO TO 25
   23 CONTINUE
   25 TBE2(5)=TBE2(I)
      TBE2(1)=TBE2(I-1)
      BE2(5)=BE2(I)
      BE2(1)=BE2(I-1)
      GO TO 21
   26 BE=BE1(I)
      GO TO 24
   22 CONTINUE
      BE=BE2(I)
   24 CONTINUE
      GAM=DARSIN(H/BE)
      ZETA=ASL-GAM-THAE
      RHO=THAE-GAM
      RE=BE/2./DSIN(THAE)
```

```
      RO=BE/(2.*DSIN(THAE)-(4.*PO*(1.-EPS**2)/E))
      CHI=CARSIN(BE/RC/2.)-GAM
      CC=A*(DSIN(B)+DSIN(THA))
      IF(THA.EQ.THAMIN)GO TO 27
      DD1=A*(1.+DSIN(THA))
      DD2=RE*(1.+DSIN(RHO))
      DD3=RC*(1.+DSIN(CHI))
      DDD=DMIN1(DD1,DD2,DD3)
      C2(2)=DDD*.99
      D2(1)=0.0
   34 CONTINUE
      STEP=(C2(2)-D2(1))/10.
      DO 39 I=1,10
      C1(I)=C2(2)-(I-1)*STEP
      D=D1(I)
      TEST2(I)=CC(A,THA)-CC(RE,RHO)+CC(RC,CHI)
      IF(DABS(TEST2(I)).LT.1.E-8)GO TO 27
      IF(TEST2(I).GT.0.0) GO TO 35
   39 CONTINUE
      D2(2)=STEP
      GO TO 34
   35 CONTINUE
      D2(2)=D1(I-1)
      D2(1)=C1(I)
   31 CONTINUE
      DO 28 I=1,5
      C1(I)=(D2(2)-D2(1))*(I-1)/4.+D2(1)
      D=D1(I)
      TEST2(I)=CC(A,THA)-CC(RE,RHO)+CC(RC,CHI)
      IF(DABS(TEST2(I)).LT.1.E-8) GO TO 29
   28 CONTINUE
      TT=0.0
      CALL INTERP(5,5,TT,C,TEST2,D1,5)
      TEST1    =CC(A,THA)-CC(RE,RHO)+CC(RC,CHI)
      IF(DABS(TEST1    ).LT.1.E-8)GO TO 27
      DO 32 I=1,4
      TT3=TEST2(I+1)*TEST2(I)
   32 IF(TT3.LT.0.0) GO TO 33
   33 D2(2)=D1(I+1)
      D2(1)=C1(I)
      GO TO 31
   29 CONTINUE
      TEST1=TEST2(I)
   27 CONTINUE
      IF(D.GT.DD) IFLAG(4)=-3
      IF(THA.GT.RHO)IFLAG(6)=-1
   99 CONTINUE
      RETURN
      END
      SUBROUTINE SINGR(C,B,N,X,Y,NF)
      IMPLICIT REAL*8(A-H,C-Z,$)
      REAL*8K,MU
      COMMON/BLK1/H,A,ZETA,OMEGA,Q,V,RC,P,ASL,RE,GAM,RHO,CHI
      COMMON/BLK2/SY,K,E,EPS,PC
      COMMON/BLK7/PRR
      IF(PRR.EQ.2.) WRITE(6,41)
   41 FORMAT(7X,'LAM',17X,'PSI',17X,'PN',18X,'TAU',17X,'FX',18X,'FY')
      STEP=B-C
      IF(STEP.LT..000001) GO TO 11
      STEP=(B-C)/N
```

```
      SUM=0.0
      SUMX=0.0
      DO 10 I=2,N,2
      ST1=C+STEP*I
      ST2=C+STEP*(I-1)
      CALL F(ST1,ST2,FY1,FX1,FY2,FX2,NF)
      SUMX=FX2+.5*FX1+SUMX
      SUM=FY2+.5*FY1+SUM
   10 CONTINUE
      STEP=STEP*A*K/3.0
      CALL F(C,B,FY1,FX1,FY2,FX2,NF)
      X=(4.0*SUMX+FX1-FX2)*STEP
      Y=(4.0*SUM+FY1-FY2)*STEP
      N=12
      RETURN
   11 X=0.
      Y=0.0
      RETURN
      END
      SUBROUTINE F(S,SS,F,G,FR,GG,NF)
      IMPLICIT REAL*8(A-H,O-Z,$)
      REAL*8K,MU
      COMMON/BLK1/H,A,ZETA,OMEGA,Q,V,RC,P,ASL,RE,GAM,RHO,CHI
      COMMON/BLK7/PRR
      GO TO (10,20),NF
   10 PSI=0.0
      PSS=0.0
      GO TO 50
   20 CALL CPSI(S,PSI)
      CALL CPSI(SS,PSS)
   50 CONTINUE
      PN=DSIN(PSI)+2.5707963267-2.*(ZETA+S)+PSI
      PS=DSIN(PSS)+2.5707963267-2.*(ZETA+SS)+PSS
      TAU=DCOS(PSI)
      TAS=DCOS(PSS)
      R=DCOS(S)*PN-DSIN(S)*TAU
      RR=DCOS(SS)*PS-DSIN(SS)*TAS
      G =DSIN(S)*PN+DCOS(S)*TAU
      GG=DSIN(SS)*PS+DCOS(SS)*TAS
      IF(PRR.EQ.1.) GO TO 30
      WRITE(6,40) SS,PSS,PS,TAS,GG,RR
      WRITE(6,40) S,PSI,PN,TAU,G,R
   40 FORMAT(1X,6E20.8)
   30 CONTINUE
      RETURN
      END
      SUBROUTINE CPSI(ST,PSI)
      IMPLICIT REAL*8(A-H,O-Z,$)
      REAL*8K,MU
      COMMON/BLK1/H,A,ZETA,OMEGA,Q,V,RC,P,ASL,RE,GAM,RHO,CHI
      X1=.625*(ST+ZETA)
      X2=X1+.1
      Y1=DSIN(X1)+2.5707963-2.*(ZETA+ST)+X1-2.5707963*DCOS(X1)
      Y2=DSIN(X2)+2.5707963-2.*(ZETA+ST)+X2-2.5707963*DCOS(X2)
    2 CONTINUE
      X=X1-Y1*(X2-X1)/(Y2-Y1)
      TL=DSIN(X)+2.5707963-2.*(ZETA+ST)+X-2.5707963*DCOS(X)
      Y2=Y1
      Y1=TL
      X2=X1
```

```
      X1=X
      IF(DABS(TL).LT..0001) GO TO 12
      GO TO 2
   12 CONTINUE
      PSI=X
      RETURN
      END
      SUBROUTINE INTERP(N,NN,XC,YO,X,Y,JJ)
      IMPLICIT REAL*8(A-H,C-Z,$)
      DIMENSION X(JJ),Y(JJ)
      YO=0.
      PU=1.
      N1=NN+1
      DO 11 I=1,N
   11 PU=PU*(XC-X(N1-I))
      DO 13 J=1,N
      PL=1.
      DO 12 I=1,N
      IF(I.EQ.J) GO TO 12
      PL=PL*(X(N1-J)-X(N1-I))
   12 CONTINUE
      PT=PU/PL/(XC-X(N1-J))
   13 YO=YO+PT*Y(N1-J)
      RETURN
      END
      SUBROUTINE GJRED(C,PT,STPT,N)
      IMPLICIT REAL*8(A-H,C-Z,$)
      DIMENSION C(4,5),STPT(5),PT(6)
      COMMON/BLK1/H,A,ZETA,OMEGA,Q,V,RC,P,ASL,RE,GAM,RHO,CHI
      COMMON/BLK5/CD
      N1=N+1
C     THIS PROGRAM PERFORMS A GAUSS-JORDAN REDUCTION
      DO 200 J=1,N
      DIV=C(J,J)
  300 S=1.0/DIV
      DO 201 K=J,N1
  201 C(J,K)=C(J,K)*S
      DO 202 I=1,N
      IF(I-J)203,202,203
  203 AIJ=-C(I,J)
      DO 204 K=J,N1
  204 C(I,K)=C(I,K)+AIJ*C(J,K)
  202 CONTINUE
  200 CONTINUE
      IF(N.LT.4)C(4,N1)=1.E-8
      IF(N.LT.3)C(3,N1)=1.E-8
      IF(DABS(C(1,N1)).GT..1) GO TO 10
      IF(DABS(C(2,N1)).GT..1) GO TO 10
      IF(DABS(C(3,N1)).GT..1) GO TO 10
      IF(DABS(C(4,N1)).GT..1) GO TO 10
      AA=1.
      GO TO 50
   10 CONTINUE
      FF=.1/DABS(C(1,N1))
      EE=.1/DABS(C(2,N1))
      HH=.1/DABS(C(3,N1))
      GG=.1/DABS(C(4,N1))
      AA=DMIN1(EE,FF,GG,HH)
   50 CONTINUE
      DO 40 I=1,N
```

```
40 STPT(I)=C(I,N1)*AA
   DO 60 I=N1,5
   STPT(I)=0.0
60 CONTINUE
   RETURN
   END
   SUBROUTINE THAMX(THAE,B,THA,BE,D,TEST1)
   IMPLICIT REAL*8(A-H,O-Z,$)
   REAL*8 K,MU
   DIMENSION IFLAG(6)
   COMMON/BLK6/IFLAG
   COMMON/BLK5/DD
   X2=THA
   Y2=D-DD
   THA=THA*.9
   CALL GECM(THAE,E,THA,BE,D,TEST1)
   Y1=D-DD
   X1=THA
 2 CONTINUE
   X=X1-Y1*(X2-X1)/(Y2-Y1)
   CALL GECM(THAE,B,X  ,BE,D,TEST1)
   Y2=Y1
   Y1=D-DD
   X2=X1
   X1=X
   IF(DABS(Y1).LT.1.E-8) GO TO 12
   GO TO 2
12 CONTINUE
   THA=X
   IFLAG(4)=-2
   RETURN
   END
   SUBROUTINE THEMN(THAE,E,THA,BE,D,TEST1)
   IMPLICIT REAL*8(A-H,O-Z,$)
   REAL*8 K,MU
   DIMENSION IFLAG(6)
   COMMON/BLK1/H,A,ZETA,OMEGA,Q,V,RC,P,ASL,RE,GAM,RHO,CHI
   COMMON/BLK6/IFLAG
   NF=1
   IF(IFLAG(2).EQ.-2) NF=2
   IF(IFLAG(4).EQ.-1.AND.NF.EQ.2) NF=3
   IF(IFLAG(1).EQ.-2.AND.NF.EQ.3) GO TO 31
   GO TO (1,2,3),NF
 1 X2=THAE
   X1=THAE*1.1
   THAE=X1
   GO TO 5
 2 X2=THA
   X1=THA*.9
   THAE=.8
   THA=X1
   NF=2
   GO TO 5
 3 X2=B
   X1=B*1.1
   THA=0.0
   THAE=0.8
   B=X1
   NF=3
 5 CONTINUE
```

```
      Y2=THA-RHO
      CALL GECM(THAE,B,THA,BE,D,TEST1)
      IF(IFLAG(5).LT.0) GO TO 30
      IF(IFLAG(3).EQ.-2.AND.NF.EQ.1) GO TO 2
      IF(IFLAG(4).EQ.-1.AND.NF.EQ.2) GO TO 3
      IF(IFLAG(1).EQ.-2.AND.NF.EQ.3) GO TO 31
      Y1=THA-RHO
   10 CONTINUE
      X=X1-Y1*(X2-X1)/(Y2-Y1)
      GO TO(6,7,8),NF
    6 THAE=X
      GO TO 9
    7 THA=X
      THAE=.8
      GO TO 9
    8 B=X
      THAE=.8
      THA=0.0
    9 CONTINUE
      CALL GECM(THAE,B,THA,BE,C,TEST1)
      IF(IFLAG(1).EQ.-2.AND.NF.EQ.3)IFLAG(5)=-2
      IF(IFLAG(5).LT.0) GO TO 30
      IF(IFLAG(3).EQ.-2.AND.NF.EQ.1) GO TO 2
      IF(IFLAG(4).EQ.-1.AND.NF.EQ.2) GO TO 3
      Y2=Y1
      Y1=THA-RHO
      X2=X1
      X1=X
      IF(CABS(Y1).LT.1.E-5) GO TO 12
      GO TO 10
   12 CONTINUE
      GO TO (13,14,15),NF
   13 THAE=X
      GO TO 16
   14 THA=X
      GO TO 16
   15 B=X
   16 CONTINUE
      IFLAG(3)=-1
   30 CONTINUE
      RETURN
   31 IFLAG(5)=-2
      RETURN
      END
$ENTRY
```

ACKNOWLEDGMENT

I would like to thank Dr. F. C. Appl for the patience and guidance which he gave so freely. I would also like to thank Kansas State University and Christensen Diamond Products Company for their assistance and financial support. A very special thanks goes to my wife who supported me in many ways.

VITA

MICHAEL ALLEN JETER

Candidate for the Degree

Master of Science

THESIS: THEORETICAL ANALYSIS OF A ROUND NOSE TOOL CUTTING AT SMALL DEPTHS

MAJOR FIELD: Mechanical Engineering

BIOGRAPHICAL:

Personal Data: Born July 1, 1953 in Wichita, Kansas; the son of David L. and Gertrude E. Jeter.

Education: Graduated from Wichita High School Southeast and the Wichita Area Vocational Technical School in 1971, I attended Wichita State University in the fall of 1971 until I transferred to Kansas State University in the fall of 1973. I received a B.S. in Mechanical Engineering in December of 1975 and completed requirements for the M.S. degree in May of 1979.

THEORETICAL ANALYSIS OF A ROUND NOSE TOOL CUTTING AT SMALL DEPTHS

by

MICHAEL A. JETER

B.S., Kansas State University, 1975

AN ABSTRACT OF A MASTER'S THESIS

Submitted in Partial Fulfillment of the

Requirements for the Degree

MASTER OF SCIENCE

Department of Mechanical Engineering

Kansas State University

Manhattan, Kansas

1979

For many years, the chip forming process in metal cutting has been approximated by an infinitely sharp tool forming a chip along a line of concentrated shear. Recently, however, it has become apparent that for small depths of cut the effect of the rounded tool tip is important. It is the object of this work to investigate the chip forming process due to the rounded portion of a tool tip cutting at very small depths. Due to the complex nature of the cutting process, the investigation took the form of a mathematical model that approximated the chip forming process.

The chip forming process was conceived to be the result of an extrusion type process where the tool and the elastic-plastic boundary act as die walls. The pressure distribution and magnitude along the tool's edge in the plastic region was determined by the use of slip-line theory while the pressure distribution and magnitude along the tool's edge in the elastic region was determined by its close relationship to an equivalent indenter. The equivalent indenter was conceived as an indenter that created the same elastic stress field in the workpiece material as the cutting process. The approximation of the equivalent indenter was dependent on the cutting process geometry and the workpiece material properties. The correct geometry for a given cutting case was determined by varying the geometry of the cutting model until the resulting force required by the equivalent indenter was the same in magnitude and direction as the resulting force required by the tool.

Although the results of the model did not duplicate experimental data sufficiently to verify the validity of the cutting model, it did match experimental data well enough to indicate some merit in the model. More importantly, when compared with a similar model, the results of the work

indicated the probable source of error. Although more research is needed before a valid model of this type can be developed, the investigation did indicate the areas needing more research.